Scaling of structure functions in homogeneous shear-flow turbulence

J. Qian

Department of Physics, Graduate School of Chinese Academy of Sciences, P.O. Box 3908, Beijing 100039, China

We apply spectral dynamics and non-Gaussian statistical model of velocity difference to study the scaling of structure functions in homogeneous shear-flow turbulence. Let L_S be the shear length scale and η the viscous scale. It is found that, when L_S/η is finite, due to a combined effect of viscosity and mean shear, the scaling deviates from normal scaling, and the deviation increases as L_S/η decreases. In the presence of a strong shear ($L_S/\eta < 100$), the deviation is substantially larger than the prediction of typical intermittency models, in agreement with recent experiments. As $L_S/\eta \to \infty$, the normal scaling is valid in the inertial range where viscous and shear effects are negligible.

I. INTRODUCTION

According to Kolmogorov [1], the fine structure of turbulence is described by structure functions. The structure function of order p is $\langle|\Delta u_r|^p\rangle$ or $\langle\Delta u_r^p\rangle$, Δu_r is the longitudinal velocity difference across a distance r, and $\langle\rangle$ means a statistical average. In the inertial range, where viscous and large-scale effects are negligible, we have scaling law $\langle|\Delta u_r|^p\rangle \sim r^{\zeta_p}$ or $\langle\Delta u_r^p\rangle \sim r^{\zeta_p}$, and ζ_p is the inertial range scaling exponent of order p [1]. The Kolmogorov 1941 theory (K41) predicts $\zeta_p = p/3$ (normal scaling), but his 1962 theory (K62) predicts that $\zeta_2 > 2/3$ and $\zeta_p < p/3$ if $p > 3$ [1,2]. Strictly speaking, Kolmogorov's inertial-range scaling is valid only in the limit of $R_\lambda \to \infty$, here R_λ is the Taylor-microscale Reynolds number. Experiments and numerical simulations are made at finite R_λ. For a finite-R_λ turbulence, we use ξ_p to represent the absolute scaling exponent of $\langle|\Delta u_r|^p\rangle$ against r, and use S_p to represent the relative scaling exponent of $\langle|\Delta u_r|^p\rangle$ against $\langle|\Delta u_r|^3\rangle$ or $D_{LLL}(r) \equiv \langle\Delta u_r^3\rangle$ by Benzi's extended self-similarity (ESS) method [3]. Experiments and numerical simulations show that ξ_p and S_p deviate from $p/3$, which have been interpreted as evidence against K41 normal scaling based on the assumption $\xi_p = \zeta_p$ and $S_p = \zeta_p$, and various intermittency models are developed to explain the deviation [2]. Since the finite Reynolds number (FRN) effects are not negligible, the scaling range observed at experimental R_λ (which is called "inertial range" in literature) is not the real inertial range [4]. In general, ξ_p and S_p are flow dependent as well as R_λ dependent, the assumption $\xi_p = \zeta_p$ and $S_p = \zeta_p$ is disputable, and the deviation of ξ_p and S_p from $p/3$ cannot be interpreted as evidence against K41 normal scaling [5]. This highlights the issue of K41 and K62.

Recently much interest and effort have been directed to study shear effects on the scaling of structure functions in turbulence (see [6–9], and references therein), and it is found that the deviation $|\xi_p\text{-}p/3|$ or $|S_p\text{-}p/3|$ is substantially larger than the prediction of typical intermittency models of K62 when there is a strong shear. In the case of wall bounded shear-flow turbulence, Benzi *et al.* [9] observed a distinct violation of the refined similarity hypothesis of K62 together with the simultaneous persistence of scaling laws. Toschi, Leveque, and Chavarria [6] pointed out that the large devia-

tion of ξ_p or $\mathbf{S}_p$ from $p/3$ (substantially larger than the prediction of typical intermittency models of K62) is a universal property of turbulence with a strong shear. How to understand the scaling behavior in shear-flow turbulence becomes an important topic of turbulence physics. The shear effect, i.e., the effect of large-scale shear motion on small-scale statistics of turbulence, is an important ingredient of FRN effects, and the study of shear effects is indispensable for settling the issue of K41 and K62.

In this paper, we apply spectral dynamics and non-Gaussian model of probability density function (PDF) of the velocity difference to study the scaling of structure functions in a homogeneous shear-flow turbulence, and the results are given in Figs. 1–5. We find that the large deviation of ξ_p or S_p from $p/3$ can be explained in the framework of K41 normal scaling ($\zeta_p = p/3$). Let η be the Kolmogorov scale, and L_S be the shear length scale at which shear and viscous effects are equal. When L_S/η is finite, due to a combined effect of viscosity and mean shear, ξ_p and S_p deviate from $\zeta_p = p/3$, and the deviation increases as L_S/η decreases. In the presence of a strong shear ($L_S/\eta < 100$), the deviation $|\xi_p\text{-}p/3|$ or $|S_p\text{-}p/3|$ is larger than the prediction of typical intermittency models of K62. In the following, we describe how the results in Figs. 1–5 are derived, and then discuss their physical meaning and some relevant issues.
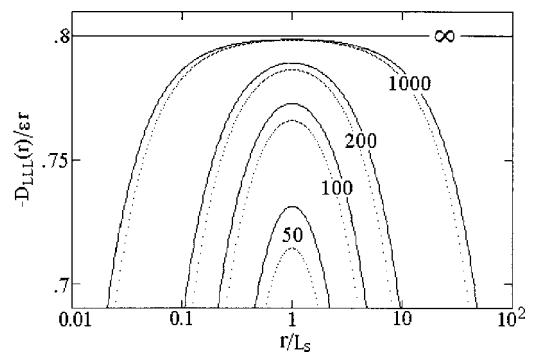
FIG. 1. $-D_{LLL}(r)/(\varepsilon r)$ vs r/L_S for $L_S/\eta = 50$, 100, 200, 1000, and ∞. L_S is shear length scale, η is Kolmogorov scale. ——, Kolmogorov constant $K_0 = 1.2$; $\cdots$ $K_0 = 1.5$. 4/5 law (9) corresponds to $L_S/\eta = \infty$.
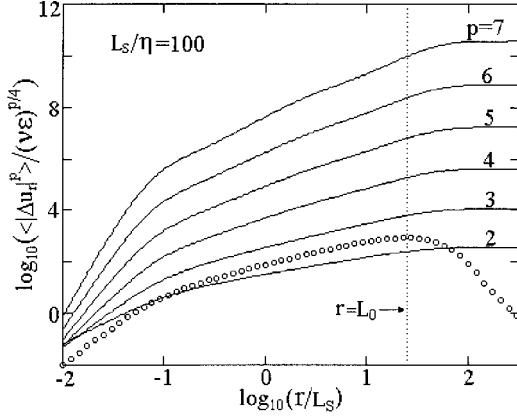
FIG. 2. Structure functions for $L_S/\eta=100$. ——
$\langle|\Delta u_r|^p\rangle/(\nu\varepsilon)^{p/4}$, $p=2$ to 7; $\circ\circ\circ$, $-D_{LLL}(r)/(\nu\varepsilon)^{3/4}$; $\cdots$, $r=L_0$ at
which $-D_{LLL}(r)$ takes its maximum.

II. SPECTRAL DYNAMIC EQUATIONS

In a real shear-flow turbulence, shear effects coexist with
other large-scale effects such as nonhomogeneous and non-
stationary effects. In this paper, we study shear effects only,
and neglect the other large-scale effects. For this purpose, we
study the simplest type of shear-flow turbulence: a homoge-
neous shear-flow turbulence. Without loss of generality, it is
supposed that the mean velocity $(U_1,0,0)$ is along the x_1
direction and there is a constant mean shear $dU_1(x_2)/dx_2$,
then we have [10]

$$\partial E(k)/\partial t + \Theta(k)dU_1(x_2)/dx_2 = T(k) - 2\nu k^2 E(k), \quad (1)$$

$$\Theta(k) = 4\pi k^2[E_{12}]_{\mathrm{av}} - 2\pi k^2[k_1\partial E_{ii}/\partial k_2]_{\mathrm{av}}. \quad (2)$$

Here ν is the kinematic viscosity, E_{ij} is the spectrum tensor,
$E_{ii}=E_{11}+E_{22}+E_{33}$ is its contraction, and $[\ ]_{\mathrm{av}}$ means
Batchelor's average. In isotropic turbulence, the correlation
and spectrum functions depend on one single scalar only,
namely, the distance r or the wave number k. That is no
longer valid in the anisotropic case. Batchelor suggested av-
eraging the correlation or spectrum functions over all direc-
tions of r or k, and then the resultant average functions de-
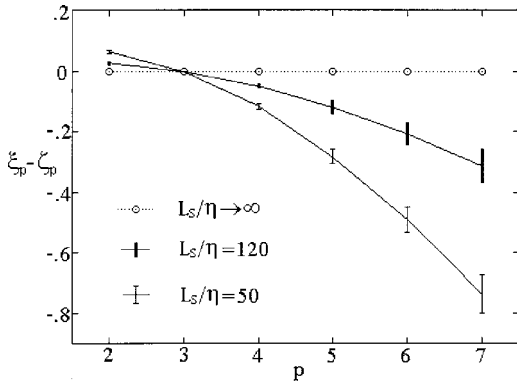
FIG. 3. ξ_p-ζ_p vs p for $L_S/\eta=50$, 120, and ∞. ξ_p is the absolute
scaling exponent, $\zeta_p=p/3$ is the inertial-range scaling exponent.
Relative scaling exponent S_p has the same behavior as ξ_p when the
ESS range is around $r=L_S$.
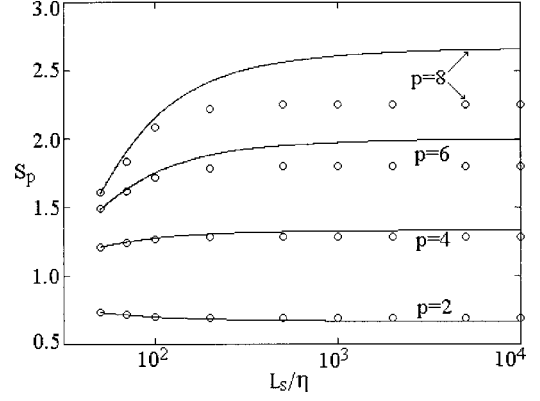
FIG. 4. Relative scaling exponent S_p vs L_S/η ($p=2$, 4, 6, and
8) over two different ESS ranges. ——, ESS range is $0.316\leq r/L_s$
≤ 3.16; $\circ\circ\circ$, ESS range is $20\leq r/\eta\leq 300$.

pend on r or k only. Many popular relations of isotropic
turbulence are also valid for these average functions [10]. In
Eq. (1), $E(k)$ is the energy spectrum and $T(k)$ is the energy
transfer spectrum. If Kolmogorov's local isotropy concept is
valid, $E(k)$ and $T(k)$ approach quantities of isotropic turbu-
lence when R_λ is high enough. In a stationary state,
$\partial E(k)/\partial t=0$, Eq. (1) becomes

$$T(k) = S\Theta(k) + 2\nu k^2 E(k), \quad S=dU_1(x_2)/dx_2. \quad (3)$$

The energy input by the mean shear S compensates the en-
ergy dissipation,
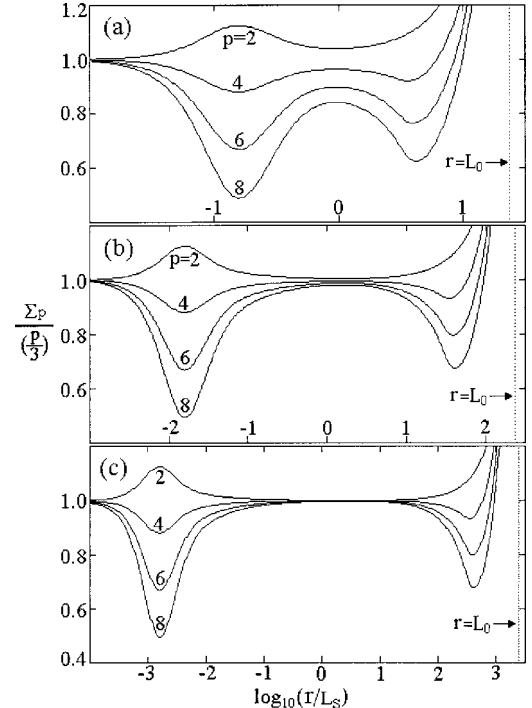
FIG. 5. $\Sigma_p/(p/3)$ vs r/L_S for $p=2$, 4, 6, and 8. Here Σ_p is the
local slope defined by Eq. (18). (a) $L_S/\eta=100$; (b) $L_S/\eta=1000$;
(c) $L_S/\eta=10^4$. $\cdots$, $r=L_0$ at which $-D_{LLL}(r)$ takes its maximum.

$$\varepsilon = 2\nu \int_0^\infty k^2 E(k)dk, \tag{4}$$

so a statistically stationary turbulence is possible [10].

The spectral equation (3) implies an energy cascade from larger scales to smaller scales, the shear term $S\Theta(k)$ plays the role of energy source, and the viscous term plays the role of energy sink. From Eq. (3), we obtain [1,10]

$$D_{LLL}(r) = -(4/5)\varepsilon r + \Psi + \Phi, \quad \Psi = 6\nu dD_{LL}(r)/dr, \tag{5}$$

$$\Phi = -12S \int_0^\infty \Theta(k)[z^2 \sin(z) + 3z \cos(z)$$
$$-3 \sin(z)]/z^5 dz, \quad z = kr. \tag{6}$$

Here Ψ and Φ represent viscous and shear effects, respectively, $D_{LL}(r) = \langle \Delta u_r^2 \rangle$ is the second-order structure function. In the universal equilibrium range, the shear effects are negligible, Eqs. (3) and (5) become

$$T(k) = 2\nu k^2 E(k), \tag{7}$$

$$D_{LLL}(r) = -(4/5)\varepsilon r + 6\nu dD_{LL}(r)/dr, \tag{8}$$

which is the Kolmogorov equation. In the inertial range, both viscous and shear terms are negligible, from Eqs. (5) or (8) we obtain Kolmogorov's 4/5 law

$$D_{LLL}(r) = -(4/5)\varepsilon r \quad \text{or} \quad -D_{LLL}(r)/(\varepsilon r) = 0.8. \tag{9}$$

III. THIRD-ORDER STRUCTURE FUNCTION IN SCALING RANGE

The scaling range of a finite-R_λ turbulence (for example observed in experiments and numerical simulations), which is usually called "inertial range" in literature, is not the real inertial range [4]. Now we derive the expression of $D_{LLL}(r)$ valid in the scaling range of a homogeneous shear-flow turbulence. Much effort has been made to study the decay of shear effect in small-scale range (see [11], and references therein), and it is found that, the shear stress cospectrum is proportional to $k^{-7/3}$ in the scaling range. Therefore, from Eqs. (2) and (6), in the scaling range we obtain (see Ref. [4])

$$\Phi/(\varepsilon r) = C_S(r/L_S)^{4/3}, \tag{10}$$

where C_S is a coefficient. It is easy to show that, in the scaling range, we have (see Ref. [4])

$$\Psi/(\varepsilon r) = C_V(r/\eta)^{-4/3}, \quad C_V = (324/55)\Gamma(4/3)K_O, \tag{11}$$

where K_O is the Kolmogorov constant and Γ is the gamma function. By definition, viscous term Ψ and shear term Φ are equal at the shear length scale L_S, so we have

$$C_S = C_V(\eta/L_S)^{4/3} = (324/55)\Gamma(4/3)K_O(\eta/L_S)^{4/3}. \tag{12}$$

In the scaling range, by Eqs. (10) and (11), Eq. (5) becomes

$$-D_{LLL}(r)/(\varepsilon r) = 0.8 - C_V(r/\eta)^{-4/3} - C_S(r/L_S)^{4/3}. \tag{13}$$

A plot of $-D_{LLL}(r)/(\varepsilon r)$ vs r/L_S is given in Fig. 1, which clearly shows that Kolmogorov's 4/5 law (9) is valid only in the limit of $L_S/\eta \to \infty$. When L_S/η is finite, $D_{LLL}(r)/(\varepsilon r)$ is not a constant, so the scaling $D_{LLL}(r) \sim r$ is not exact. By using Eqs. (11)–(13), we find that $-D_{LLL}(r)/(\varepsilon r)$ attains its maximum at $r = L_S$, and the maximum is

$$[-D_{LLL}(r)/(\varepsilon r)]_{\max} = 0.8 - 2C_V(L_S/\eta)^{-4/3}. \tag{14}$$

Obviously the scaling range is around $r = L_S$, where $-D_{LLL}(r)/(\varepsilon r)$ changes with r slowly, and the scaling $D_{LLL}(r) \sim r$ is approximately valid.

According to Fig. 1 and Eq. (14), strictly speaking, Kolmogorov's 4/5 law (9) is not valid in the scaling range around $r = L_S$ when L_S/η is finite. Therefore, the scaling range (which is usually called "inertial range" in literature) is not the real inertial range. Only in the limit of $L_S/\eta \to \infty$, the scaling range becomes the inertial range where viscous and shear effects are absent and Kolmogorov's 4/5 law (9) is valid.

IV. CALCULATE STRUCTURE FUNCTIONS BY NON-GAUSSIAN STATISTICAL MODEL

With some modifications, the mathematical procedure developed in Ref. [5] can be applied here to calculate structure function $\langle |\Delta u_r|^p \rangle$. The main modification is that here $D_{LLL}(r)$ should satisfy Eq. (13) in the scaling range around $r = L_s$. The outline of the mathematical procedure of calculating $\langle |\Delta u_r|^p \rangle$ is as follows. For a given L_S/η, first we use (7), (8), and (13) to determine $D_{LL}(r)$ and $D_{LLL}(r)$, then by using a non-Gaussian PDF model of the velocity difference, we calculate high-order structure functions. A systematic justification of the non-Gaussian PDF model of velocity difference is given in Ref. [5]. Let $P(x)$ be the PDF of normalized velocity difference $x = |\Delta u_r|/D_{LL}(r)^{1/2}$, and we have

$$\langle |\Delta u_r|^p \rangle = D_{LL}(r)^{p/2} \langle x^p \rangle, \quad \langle x^p \rangle = \int_0^\infty x^p P(x)dx. \tag{15}$$

The tail of $P(x)$ has the form of stretched exponentials [5],

$$P(x) = P_0 \exp(-Bx^\mu) \quad \text{while} \quad x > 2, \tag{16}$$

here μ is the stretching exponent. As r decreases from the large scale to the viscous scale, μ decreases from 2 to around 0.5. For small r, $P(x)$ is far from Gaussian, and intersects with Gaussian PDF

$$P_G(x) = (2/\pi)^{1/2} \exp(-x^2/2), \quad 0 \leq x < \infty$$

at two points x_1 and x_2. Hence $P(x_1) = P_G(x_1)$ and $P(x_2) = P_G(x_2)$, $x_1 < 1$ and $2 < x_2$ [5]. Let $P(x) = \exp[-f(x)]$, $f(x)$ is fitted by low-order polynomials over the narrow intervals $0 \leq x \leq x_1$ and $x_1 \leq x \leq x_2$. The coefficients of these polynomials are determined by the cubic spline method and some conditions at $x = 0$, so $P(x)$ are completely determined by

the four parameters B, μ, x_1, and x_2, which depend on the distance r. The r dependence of B, μ, x_1, and x_2 are determined by the following four conditions: $\langle x^0 \rangle = 1$, $\langle x^2 \rangle = 1$, $\langle x^3 \rangle = \langle |\Delta u_r|^3 \rangle / D_{LL}(r)^{3/2}$, and $\langle x^6 \rangle = C \langle x^4 \rangle^{\alpha}$. Here C is a coefficient, and the exponent α is around 2.8 [5]. By the relation $\langle |\Delta u_r|^3 \rangle \sim D_{LLL}(r)$ that is valid in the dissipation range and the scaling range, and the asymptotic condition $\langle |\Delta u_r|^3 \rangle \rightarrow 2(2/\pi)^{1/2} D_{LL}(r)^{3/2}$ as $r \rightarrow \infty$, we determine $\langle |\Delta u_r|^3 \rangle$ from $D_{LL}(r)$ and $D_{LLL}(r)$. While the $P(x)$ is determined, by using Eq. (15) we calculate $\langle |\Delta u_r|^p \rangle$. As an illustration, Fig. 2 shows the structure functions obtained in this way for the case of $L_S / \eta = 100$. In order to save the reader from having to look up previous papers, a description of the non-Gaussian PDF model is given in the Appendix.

V. SCALING EXPONENTS. LONG-RANGE VISCOUS AND SHEAR EFFECTS

So long as $\langle |\Delta u_r|^p \rangle$ is obtained by the mathematical procedure described above, we can calculate the scaling exponents ξ_p and S_p. The log-log plot of $\langle |\Delta u_r|^p \rangle$ against r within the scaling range is fitted by a straight line using the least-square method, and its slope is the absolute scaling exponent ξ_p. While L_S / η is finite, the scaling $\langle |\Delta u_r|^p \rangle \sim r^{\xi_p}$ is not exact, and ξ_p depend on how to define the scaling range. In this paper, the scaling range $r_1 \leqslant r \leqslant r_2$ is around the maximum point of $-D_{LLL}(r)/(\varepsilon r)$, and is defined as the widest range satisfying the following conditions:

absolute scaling exponent of $D_{LLL}(r)$ over

$$r_1 \leqslant r \leqslant r_2 \text{ is equal to } 1, \tag{17a}$$

$$-D_{LLL}(r)/\varepsilon r \geqslant C[-D_{LLL}(r)/\varepsilon r]_{max}$$

$$\text{when } r_1 \leqslant r \leqslant r_2, \quad C < 1. \tag{17b}$$

The smaller C is, the wider the scaling range is, and the worse the quality of the scaling is. Figure 3 shows the deviation of absolute scaling exponent ξ_p from inertial-range scaling exponent ζ_p for $L_S / \eta = 50$, 120, and ∞, and the "error bar" corresponds to C changing from 0.9 to 0.9999. Since $\langle |\Delta u_r|^3 \rangle \sim D_{LLL}(r)$ in the scaling range $r_1 \leqslant r \leqslant r_2$, we have $\xi_3 = 1$ over the range, so the relative scaling exponent of $\langle |\Delta u_r|^p \rangle$ against $\langle |\Delta u_r|^3 \rangle$ [or $-D_{LLL}(r)$] over the range will have the same behavior as ξ_p shown in Fig. 3. The relative scaling exponent S_p is determined by Benzi's ESS method [3], and depends upon the limits of the ESS range. In Fig. 4, we show S_p over two different ESS ranges. The first ESS range is around $r = L_s$ ($0.316 \leqslant r/L_s \leqslant 3.16$), the resultant S_p approach the inertial-range scaling exponent $\zeta_p = p/3$ as $L_S / \eta \rightarrow \infty$. The second ESS range is $20 \leqslant r/\eta \leqslant 300$, which is suggested by Arneodo *et al.* [12], and S_p deviates from $\zeta_p = p/3$ even in the limit of $L_S / \eta \rightarrow \infty$.

It is interesting to explore the physical meaning of the results of Figs. 3 and 4. For this purpose, the local slope of the log-log plot of $\langle |\Delta u_r|^p \rangle$ against $-D_{LLL}(r)$,

$$\Sigma_p = d \log_{10}(\langle |\Delta u_r|^p \rangle) / d \log_{10}[-D_{LLL}(r)], \tag{18}$$

is shown in Fig. 5 for $L_S / \eta = 10^2$, 10^3, and 10^4. When $r/L_S \rightarrow 0$, $-D_{LLL}(r) \sim r^3$, and $\langle |\Delta u_r|^p \rangle \sim r^p$, so $\Sigma_p \rightarrow p/3$ as $r/L_S \rightarrow 0$. When $r/L_S \rightarrow \infty$, $\langle |\Delta u_r|^p \rangle$ approaches a positive constant, but $-D_{LLL}(r) \rightarrow 0$, so $\Sigma_p \rightarrow \infty$ as $r \rightarrow L_0$ as shown in Fig. 5, here L_0 is the r value at which $-D_{LLL}(r)$ takes its maximum. We have $L_0 / \eta \sim (L_S / \eta)^2$ and $R_\lambda \sim (L_0 / \eta)^{2/3}$. As shown in Fig. 5(c), the viscous effect increases Σ_2 and decreases Σ_p ($p > 3$), giving rise to a positive bump for Σ_2 and negative bumps for Σ_p ($p > 3$) over the range $1 < r/\eta < 10^4$. Similarly the shear effect increases Σ_2 and decreases Σ_p ($p > 3$) in the range $r/L_0 < 0.1$. Figure 5 shows that viscous and shear effects are of long range. When L_S / η is finite, the range of viscous effect and the range of shear effect penetrate into each other [the penetration is obvious in Figs. 5(a) and 5(b)], and the combination of the viscous and shear effects leads to an increase in Σ_2 and a decrease in Σ_p ($p > 3$) in the scaling range around $r = L_S$. The scaling exponents ξ_p and S_p are equal to some mean value of the local slope Σ_p. Hence, the deviation of ξ_p and S_p from the inertial-range scaling exponent $\zeta_p = p/3$ shown in Figs. 3 and 4 is a combined effect of viscosity and mean shear, and increases as L_S / η decreases.

VI. DISCUSSION AND SUMMARY

As mentioned above, Fig. 5 clearly shows that the viscous effect is not negligible in the range $20 \leqslant r/\eta \leqslant 300$ due to it being of long range. This explain why the S_p over range $20 \leqslant r/\eta \leqslant 300$ deviates from $\zeta_p = p/3$ even in the limit of $L_S / \eta \rightarrow \infty$ (see Fig. 4): although the shear effects is negligible in the range $20 \leqslant r/\eta \leqslant 300$ while $L_S / \eta \rightarrow \infty$, the viscous effect cannot be neglected. The so-called homogeneous isotropic turbulence (HIT) data of S_p reported in Ref. [3] deviate substantially from $p/3$, and do not correspond to the limit case of $L_S / \eta \rightarrow \infty$ ($L_0 / \eta \rightarrow \infty$ and $R_\lambda \rightarrow \infty$). In these HIT measurements, although the mean shear is negligible at measurement points (at the axis of a jet flow or in the core region of a wall turbulence), there are other large-scale effects due to the macrostructure of the flows being not homogeneous and stationary, and the ESS range is within $4 < r/\eta < 10^3$ [3,12], where the viscous and large-scale effects are not negligible. Hence these HIT data of S_p deviate substantially from the inertial-range scaling exponent $\zeta_p = p/3$ [5].

Recently, interesting work [13] has been done to disentangle ζ_p from effects of large-scale shear motion. Arad *et al.* [13] apply an SO(3) symmetry group method to analyze data of atmospheric boundary layer (ABL) flow at $R_\lambda = 10^4$. They adopt the assumption of cylindrical symmetry about the mean-wind direction and obtain $\zeta_2 = 0.69$ if ζ_2 is equal to their leading scaling exponent in the isotropic sector. Kurien *et al.* [13] apply the same method but do not assume cylindrical symmetry, and obtain $\zeta_2 = 0.68$. The result $\zeta_2 = 0.68$ of Kurien *et al.* (smaller than 0.69 of Arad *et al.*) is nearer the K41 value 0.67 than the K62 value 0.70. They have largely disregarded the inhomogeneity of ABL flow. Supposing we know how to take into account the inhomogeneity of the ABL flow and the ABL flow is at higher $R_\lambda = 10^6$, it is not absurd to expect that $\zeta_2 = 0.67$ will possibly be obtained,

which favors Kolmogorov's 2/3 law rather than the K62 anomalous scaling ($\zeta_2 = 0.70$).

Finally we summarize. We apply spectral dynamics and non-Gaussian PDF model of velocity difference to study the scaling of structure functions in a homogeneous shear-flow turbulence. From Fig. 5, it is clear that viscous and shear effects are of long range. When L_S/η is finite, due to a combined effect of viscosity and mean shear, Kolmogorov's 4/5 law (9) is not valid in the scaling range around $r = L_S$ (see Fig. 1), and the scaling exponents ξ_p (or S_p) deviate from the inertial-range scaling exponent $\zeta_p = p/3$ (see Figs. 3 and 4). The deviation $|\xi_p - p/3|$ or $|S_p - p/3|$ increases as L_S/η decreases, and is larger than the prediction of typical intermittency models of K62 while there is a strong shear ($L_S/\eta < 100$). As $L_S/\eta \to \infty$, the scaling range around $r = L_S$ becomes the inertial range, where Kolmogorov's 4/5 law (9) and K41 normal scaling ($\zeta_p = p/3$) are valid. Therefore, we demonstrate that the anomalous scaling, observed in a shear-flow turbulence as well as in HIT, can be explained in the framework of K41 normal scaling ($\zeta_p = p/3$), without appealing to K62 theory. This author do not intend to revive K41 in its entirety, so we do not use the simple dimensional argument of K41 to derive the inertial-range scaling exponents. In this author's opinion, the pearls of K41 are Kolmogorov's 4/5 law for $D_{LLL}(r)$ and 2/3 law for $D_{LL}(r)$ (or $-5/3$ law for energy spectrum), which are valid in the real inertial range of homogeneous isotropic turbulence. The 4/5 law is an exact statistical result of Navier-Stokes (NS) equations [1], and the $-5/3$ law of energy spectrum can be derived from NS equations by reasonable statistical closure methods ([14], and references therein). Based upon the 4/5 law and the $-5/3$ law, we apply the non-Gaussian PDF model of velocity difference to obtain high-order scaling exponents [5].

APPENDIX: NON-GAUSSIAN PROBABILITY DENSITY FUNCTION (PDF) MODEL

Suppose $D_{LL}(r)$ and $D_{LLL}(r)$ have been determined by solving spectral dynamic equations or other methods [5]. If $P(x)$ is known, we can use Eq. (15) to calculate the structure function $\langle |\Delta u_r|^p \rangle$. Although we are not able to drive the expression of $P(x)$ from the Navier-Stokes equations, we know the basic properties of $P(x)$, which can be applied to derive the form of $P(x)$. The tail of $P(x)$ can be well fitted by stretched exponentials of the form [15],

$$P(x) = P_0 \exp(-Bx^\mu) \quad \text{while} \quad x > 2, \qquad (A1)$$

and the parameters P_0, B, and μ are functions of r. The stretching exponent μ decreases from 2 to around 0.5 as the distance r decreases from the large scale L to the Kolmogorov scale η. The PDF of the absolute value of a Gaussian random variable is

$$P_G(x) = (2/\pi)^{1/2} \exp(-x^2/2) \quad 0 \leq x < \infty. \qquad (A2)$$

By the definition of $P(x)$ and $P_G(x)$, we have

$$\int_0^\infty P(x)dx = \int_0^\infty P_G(x)dx = 1 \qquad (A3)$$

and

$$\int_0^\infty x^2 P(x)dx = \int_0^\infty x^2 P_G(x)dx = 1. \qquad (A4)$$

When r is in the small-scale range, the $P(x)$ is far from Gaussian, having a shape characteristic of a strongly intermittent random variable: the $P(x)$ of very small x and very large x is considerably greater than the corresponding Gaussian $P_G(x)$, while the $P(x)$ of intermediate x is smaller than $P_G(x)$. Hence $P(x)$ and $P_G(x)$ intersect at two points x_1 and x_2,

$$P(x_1) = P_G(x_1) \quad \text{and} \quad P(x_2) = P_G(x_2). \qquad (A5)$$

Our numerical calculations indicate that $x_1 < 1$ and $2 < x_2 < 3$, which is in agreement with experimental data [15]. By Eqs. (A2) and (A5), the parameter P_0 in (A1) can be expressed in terms of x_2, B, and μ,

$$P_0 = (2/\pi)^{1/2} \exp(Bx_2^\mu - x_2^2/2). \qquad (A6)$$

When the four parameters x_1, x_2, B, and μ in Eqs. (A1) and (A5) are known, the $P(x)$ of large x ($x \geq x_2 > 2$) can be calculated by using Eqs. (A1) and (A6), and the $P(x)$ of small x ($x < x_2$) can be determined by proper boundary condition at $x = 0$ and the mathematical conditions of continuity and smoothness.

Let $f(x) = -\ln[P(x)]$, $f(x)$ changes with x much slower than $P(x)$. Since $P(x)$ should become the stretching exponentials (A1) for large x, we have

$$P(x) = \exp[-f(x)], \qquad (A7)$$

$$f(x) = -\ln(P_0) + Bx^\mu = -\ln[(2/\pi)^{1/2}] + x_2^2/2$$
$$+ B(x^\mu - x_2^\mu) \quad \text{if} \quad x \geq x_2. \qquad (A8)$$

Hence we only need to fit $P(x)$ or $f(x)$ over the interval $0 \leq x \leq x_2$. In order to reduce the fitting error, we divide the interval $0 \leq x \leq x_2$ into two smaller subintervals, i.e., $0 \leq x \leq x_1$ and $x_1 \leq x \leq x_2$. Since $f(x)$ change with x smoothly and slowly, it is reasonable to use a low-order polynomial to fit $f(x)$ over the narrow intervals $0 \leq x \leq x_1$ and $x_1 \leq x \leq x_2$, so we have

$$f(x) = A_0 + A_1 x + A_2 x^2 + A_3 x^3 \quad \text{if} \quad x_1 \leq x \leq x_2, \quad (A9)$$

$$f(x) = B_0 + B_1 x + B_2 x^2 + B_3 x^3 \quad \text{if} \quad 0 \leq x \leq x_1. \quad (A10)$$

$P(x)$ and $f(x)$ are continuous and smooth at x_1 and x_2. Following the cubic spline method of applied mathematics, by using Eq. (A5) and some proper boundary condition at $x = 0$, the coefficients A_i and B_i ($i = 0, 1, 2, 3$) in Eqs. (A9) and (A10) can be calculated so long as the parameters B, μ, x_1, and x_2 are known. Therefore, the $P(x)$ have four indepen-

dent parameters B, μ, x_1, and x_2 only, other parameters A_i and B_i ($i=0,1,2,3$) can be expressed in terms of them.

Various boundary condition (BC) at $x=0$ have been tried and compared. Three typical boundary conditions are

$$B_3=0 \quad \text{and no BC is needed at } x=0, \quad \text{(A11a)}$$

$$df(x)/dx=0 \quad \text{at } x=0, \quad \text{(A11b)}$$

$P(0)$ or $f(0)$ is given by some empirical formula.

$$\text{(A11c)}$$

By using experimental data of Tabeling *et al.* [15], it is easy to determine how $f(0)$ and μ change with r, and then to obtain the empirical formula of (A11c). Our numerical calculations show that different boundary conditions lead to the same behavior of the high-order scaling exponents (see Ref. [5]).

When the four independent parameters B, μ, x_1, and x_2 are determined, we can use Eq. (15) to calculate the structure function $\langle|\Delta u_r|^p\rangle$. Four independent conditions are needed to determine the four parameters B, μ, x_1, and x_2. We already have two conditions (A3) and (A4), we need two more conditions. The third condition is

$$\langle|\Delta u_r|^3\rangle/D_{LL}(r)^{3/2}=\langle x^3\rangle=\int_0^\infty x^3 P(x)dx. \quad \text{(A12)}$$

In the scaling range $\eta\ll r\ll L$ of finite- R_λ turbulence, $\langle|\Delta u_r|^p\rangle\sim r^{\xi_p}$, so we have

$$\langle x^n\rangle=C\langle x^m\rangle^{\alpha(n,m)}, \quad x=|\Delta u_r|/D_{LL}(r)^{1/2}, \quad \text{(A13)}$$

$$\xi_n-n\xi_2/2=\alpha(n,m)(\xi_m-m\xi_2/2). \quad \text{(A14)}$$

Here C is a coefficient. For example, in the case of $n=6$ and $m=4$, the exponent $\alpha(6,4)$ is around 2.8. When r approaches the large scale L, the $P(x)$ approaches the Gaussian $P_G(x)$, and $\langle x^m\rangle$ approaches $G(m)\equiv\int_0^\infty x^m P_G(x)dx$, $G(3)=2(2/\pi)^{1/2}$, $G(4)=3$, $G(5)=8(2/\pi)^{1/2}$, $G(6)=15$, and so on. The stretching exponent μ is equal to 2 for the Gaussian $P_G(x)$. A convenient way of determining the coefficient C in (A13) is by the requirement that $\langle x^n\rangle\rightarrow G(n)$ and $\langle x^m\rangle\rightarrow G(m)$ as $\mu\rightarrow2$. In fact, the behavior of scaling exponents does depend upon how to determine C, so we can choose a convenient way. With a particular choice of (n,m), for example $(n,m)=(6,4)$, Eq. (A13) is the fourth condition. The four conditions (A3), (A4), (A12), and (A13) are used to determined the four independent parameters B, μ, x_1, and x_2 of the $P(x)$. In this way, we can determine how the $P(x)$ changes with the distance r for any given R_λ, so long as we know the second and third structure functions $D_{LL}(r)$ and $\langle|\Delta u_r|^3\rangle$. For more topics of the non-Gaussian PDF model, e.g. how to determine $\langle x^3\rangle\equiv\langle|\Delta u_r|^3\rangle/D_{LL}(r)^{3/2}$ in third condition (A12), the consistency problem of different choices of (n,m) in (A13), and the validity of fourth condition (A13) over the whole range $0.5\leq\mu\leq2$ due to the important property of general similarity of the PDF model, please see [5].

[1] A. N. Kolmogorov, C. R. Acad. Sci. URSS **30**, 301 (1941); J. Fluid Mech. **13**, 82 (1962); A. S. Monin and A. M. Yaglom, *Statistical Fluid Mechanics* (Cambridge University Press, Cambridge, 1975).

[2] U. Frisch, *Turbulence: The Legacy of A. N. Kolmogorov* (Cambridge University Press, Cambridge, 1995); K. R. Sreenivasan and R. A. Antonia, Annu. Rev. Fluid Mech. **29**, 435 (1997).

[3] R. Benzi, S. Ciliberto, R. Tripiccione, C. Baudet, F. Massaioli, and S. Succi, Phys. Rev. E **48**, R29 (1993); R. Benzi, S. Ciliberto, C. Baudet, and G. R. Chavarria, Physica D **80**, 385 (1995).

[4] J. Qian, Phys. Rev. E **55**, 337 (1997); **60**, 3409 (1999).

[5] J. Qian, Phys. Rev. E **58**, 7325 (1998); J. Phys. A **31**, 3193 (1998); Phys. Rev. Lett. **84**, 646 (2000); Int. J. Mod. Phys. B **15**, 1085 (2001).

[6] F. Toschi, E. Leveque, and G. R. Chavarria, Phys. Rev. Lett. **85**, 1436 (2000).

[7] M. Onorato, R. Canussi, and G. Iuso, Phys. Rev. E **61**, 1447 (2000).

[8] F. Toschi, G. Amati, S. Succi, R. Benzi, and R. Piva, Phys. Rev. Lett. **82**, 5044 (1999).

[9] R. Benzi, G. Amati, C. M. Casciola, F. Toschi, and R. Piva, Phys. Fluids **11**, 1284 (1999).

[10] J. O. Hinze, *Turbulence*, 2nd ed. (McGraw-Hill, New York, 1975); G. K. Batchelor, *The Theory of Homogeneous Turbulence* (Cambridge University Press, New York, 1953).

[11] S. G. Saddoughi and S. V. Veeravalli, J. Fluid Mech. **268**, 333 (1994).

[12] A. Arneodo *et al.*, Europhys. Lett. **34**, 411 (1996).

[13] I. Arad, B. Dhruva, S. Kurien, V. S. L'vov, I. Procaccia, and K. R. Sreenivasan, Phys. Rev. Lett. **81**, 5330 (1998); K. R. Sreenivasan and B. Dhruva, Prog. Theor. Phys. Suppl. **130**, 103 (1998); S. Kurien, V. S. L'vov, I. Procaccia, and K. R. Sreenivasan, Phys. Rev. E **61**, 407 (2000); L. Biferale and F. Toschi, Phys. Rev. Lett. **86**, 4831 (2001).

[14] J. Qian, Phys. Fluids **26**, 2098 (1983).

[15] P. Tabeling, G. Zocchi, F. Belin, J. Maurer, and H. Willaime, Phys. Rev. E **53**, 1613 (1996); P. Kailasnath, K. R. Sreenivasan, and G. Stolovitzky, Phys. Rev. Lett. **68**, 2766 (1992); B. Castaing, Y. Gagne, and E. Hopfinger, Physica D **46**, 177 (1990).